The regulation of polyamine pathway proteins in models of skeletal muscle hypertrophy and atrophy: a potential role for mTORC1

The Regulation of Polyamine Pathway Proteins in Models of Skeletal Muscle Hypertrophy and Atrophy – a potential role for mTORC1

Michael Tabbaa[1,2*], Tania Ruz Gomez[1,2*], Dean G. Campelj[1,2], Paul Gregorevic[3,4,5], Alan Hayes[1,2,6] and Craig A. Goodman[1,2,3]

*These authors contributed equally to this project

Affiliations:

[1]Institute for Health and Sport (iHeS), Victoria University, Melbourne, Australia

[2]Australian Institute for Musculoskeletal Science (AIMSS), Victoria University, St Albans, Victoria, Australia.

[3]Centre for Muscle Research (CMR), Department of Physiology, The University of Melbourne, Parkville, Victoria, Australia.

[4]Department of Biochemistry and Molecular Biology, Monash University, Clayton, Victoria, Australia.

[5]Department of Neurology, The University of Washington School of Medicine, Seattle, USA.

[6]Department of Medicine - Western Health, Melbourne Medical School, The University of Melbourne, Melbourne, Victoria, Australia

Running Head:

Polyamine Pathway Proteins in Muscle Hypertrophy and Atrophy

Correspondence:

Craig A. Goodman
Centre for Muscle Research
Department of Anatomy and Physiology
School of Biomedical Sciences
Faculty of Medicine Dentistry and Health Sciences
Level 5, W504, Medical Building 181
Cnr of Royal Pde and Grattan St
The University of Melbourne, Parkville, Victoria 3010 Australia
Email: craig.goodman@unimelb.edu.au

Abstract

Polyamines have been shown to be absolutely required for protein synthesis and cell growth. The serine/threonine kinase, the mechanistic target of rapamycin complex 1 (mTORC1), also plays a fundamental role in the regulation of protein turnover and cell size, including in skeletal muscle, where mTORC1 is sufficient to increase protein synthesis and muscle fiber size, and is necessary for mechanical overload-induced muscle hypertrophy. Recent evidence suggests that mTORC1 may regulate the polyamine metabolic pathway; however, there is currently no evidence in skeletal muscle. This study examined changes in polyamine pathway proteins during muscle hypertrophy induced by mechanical overload (7 d), with and without the mTORC1 inhibitor, rapamycin, and during muscle atrophy induced by food deprivation (48 h) and denervation (7 d) in mice. Mechanical overload induced an increase in mTORC1 signalling, protein synthesis and muscle mass, and these were associated with rapamycin-sensitive increases in adenosylmethione decarboxylase 1 (Amd1), spermidine synthase (SpdSyn) and c-Myc. Food deprivation decreased mTORC1 signalling, protein synthesis and muscle mass, accompanied by a decrease in spermidine/spermine acetyltransferase 1 (Sat1). Denervation, resulted increased mTORC1 signalling and protein synthesis, and decreased muscle mass, which was associated with an increase in SpdSyn, spermine synthase (SpmSyn) and c-Myc. Combined, these data show that polyamine pathway enzymes are differentially regulated in models of altered mechanical and metabolic stress, and that Amd1 and SpdSyn are, in part, regulated in a mTORC1-dependent manner. Furthermore, these data suggest that polyamines may play a role in the adaptive response to stressors in skeletal muscle.

Introduction

Skeletal muscle mass is thought to be broadly regulated by the net difference between the global rates of protein synthesis and protein degradation, with net increases in protein degradation eventually leading to reduced muscle mass (i.e. muscle atrophy), while net increases in protein synthesis leads to muscle growth (i.e. muscle hypertrophy) (29).

Protein synthesis predominantly involves the cap-dependent translation of mRNAs in a complex process that relies on numerous translation initiation and elongation factors, as well as ribosomes and ribosome-associated proteins (22). Protein synthesis is predominantly regulated at the level of translation initiation and a major regulator of translation initiation is the multi-protein serine/threonine kinase complex known as the mechanistic target of rapamycin complex 1 (mTORC1) (22). mTORC1 regulates cap-dependent translation initiation, in part, by the direct phosphorylation, and subsequent activation and inhibition, of downstream targets, such as $p70^{S6K1}$ and 4E-BP1, respectively (22). Furthermore, many, but not all, of mTORC1's downstream effects are inhibited by the drug, rapamycin (34). Importantly, mTORC1 activation is known to disproportionately increase the translation of some mRNAs more so than others, such as 5'-tract of pyrimidine (5'-TOP) mRNAs that typically encode for translation initiation and elongation factors and ribosomal proteins (42). Another class of mRNAs whose translation has the potential to be positively regulated by mTORC1 activation are mRNAs with highly structured guanine/cytosine (G-C)-rich 5'-UTRs, such as those that encode for cell growth and pro-survival proteins, including Bcl-2, BCL-xL, IGF-II, cyclin D1 and c-Myc [for review see (11)]. Included in this group is the mRNA of the growth-related protein, ornithine decarboxylase (Odc1), a key component of the polyamine synthesis pathway (9).

Odc1 catalyzes the first rate-limiting reaction of the polyamine pathway in which ornithine is decarboxylated to produce putrescine [for review see (4)]. Putrescine is then converted to spermidine (Spd) by spermidine synthase (SpdSyn), a reaction that requires an aminopropyl donor, in the form of decarboxylated *S*-adenosylmethionine (dcAdoMet or dcSAM) which is provided by the enzymatic reaction catalyzed by *S*-adenosylmethionine decarboxylase (AdoMetDC; aka Amd1) (4). In turn, Spd can then be converted to spermine (Spm) by spermine synthase (SpmSyn), with the required aminopropyl group again being supplied by the Amd1 catalysed reaction. Spm can also be converted back to Spd via the enzyme, spermine oxidase (Smox), while Spd and Spm can both be acetylated and removed from the pathway via the action of spermidine/spermine N^1-acetyltransferase (Sat1) (4). Importantly, polyamines are absolutely essential for normal cell function, with depletion of polyamines leading to complete inhibition of protein synthesis and cell

84 growth (40). Furthermore, there is mounting evidence that mTORC1 may directly, or indirectly,
85 regulate aspects of the polyamine pathway [for review see (44)].

86 One of the earliest studies suggesting a potential link between mTORC1 and the polyamine pathway
87 found that Odc1 activity in cultured non-muscle cells was increased by serum stimulation and this
88 increase was inhibited by rapamycin (52). Evidence of a more direct role for mTORC1 in polyamine
89 synthesis comes from a recent study showing that mTORC1 directly phosphorylates Amd1 leading to
90 reduced proteasome-mediated Amd1 degradation in prostate cancer cells (63). Another potential
91 link between mTORC1 and the polyamine pathway is that similar to Odc1, the 5'-UTR of the mRNA
92 encoding SpdSyn also has a high G-C content and is predicted to form extensive secondary structure
93 that impairs ribosomal scanning and, therefore, translation initiation (35, 58). As such, mTORC1-
94 mediated activation of cap-dependent translation, the recruitment of the eIF4A RNA helicase and
95 the $p70^{S6K1}$-mediated phosphorylation of eIF4B (41), may also facilitate SpdSyn mRNA translation
96 and promote Spd synthesis. mTORC1 activation also increases the translation of the transcription
97 factor, c-Myc (8), and the genes for Odc1, Amd1 and SpdSyn are known to also be transcriptionally
98 regulated by c-Myc (1, 17-19). Thus, mTORC1 could also indirectly increase the expression of Odc1,
99 Amd1 and SpdSyn via a c-Myc-dependent mechanism.
100
101 Despite the growing body of evidence supporting a role for mTORC1 as a regulator of the polyamine
102 pathway, to date, there is currently no direct evidence of a role for mTORC1 in the regulation of key
103 polyamine pathway proteins in skeletal muscle. Nonetheless, there is some data suggesting that
104 changes in polyamine metabolism may play a role in muscle adaptation in health and disease. For
105 example, Smox protein was recently shown to be downregulated in skeletal muscle during muscle
106 atrophy associated with immobilization, fasting, denervation and aging (2). Smox and Amd1 proteins
107 were also recently found to be downregulated in a mouse model of LAMA2-deficient congenital
108 muscular dystrophy (36). Additionally, Amd1 and Odc1 gene expression are known to be positively
109 regulated in skeletal muscle by androgens and androgen receptor agonists (15, 38, 39, 49). As
110 further evidence of a potential role for polyamine metabolism in muscle, we recently found that
111 SpdSyn protein, but not mRNA, was upregulated in a mouse model of follistatin (FST)-induced
112 muscle hypertrophy (10), supporting the hypothesis that SpdSyn protein is, in part, regulated at the
113 level of translation during growth in skeletal muscle. Interestingly, the increase in SpdSyn occurred
114 after only 2 d of FST induction and remained elevated for at least 4 wk as muscle continued to
115 undergo hypertrophy (10), showing that the increase in SpdSyn is a relatively early event in this
116 hypertrophic model. Given that FST-induced muscle hypertrophy is associated with an increase in
117 mTORC1 signalling, and that rapamycin markedly inhibits FST-induced growth (61), these data

support the idea that SpdSyn protein expression may, in part, be regulated by a mTORC1-dependent mechanism; however, to date, this hypothesis has not been directly tested in models of adaptive muscle growth.

Therefore, the overall aim of this study was to investigate changes in the expression of polyamine pathway proteins in models of skeletal muscle hypertrophy (i.e. mechanical overload) and atrophy (i.e. denervation and food deprivation). Secondly, we aimed to specifically examine whether SpdSyn would be upregulated during mechanical overload-induced muscle hypertrophy and, if so, whether the increase in SpdSyn protein would be inhibited by the mTORC1 inhibitor, rapamycin.

Methods

Animals

Female FVB/N mice, aged 8-11 wk, were purchased from Animal Resources Centre (ARC; Western Australia) and housed at the Western Centre for Health, Research and Education (Sunshine Hospital, Victoria, Australia) on a 12 h light/dark cycle with *ad libitum* access to food and water. All surgeries were performed under isoflurane anesthesia, and following tissue extraction, mice were killed by cervical dislocation while still under anesthesia. All experimental procedures were approved by the Victoria University Animal Ethics Committee (VUAEC #16-006 and #19-001) and conformed to the *Australian Code of Practice for the Care and Use of Animals for Scientific Purposes, 8th Edition, 2003.*

Mechanical overload

To examine the effects of mechanical overload-induced muscle hypertrophy, mice were anesthetized with isoflurane and immediately prior to the surgery mice were given an intraperitoneal (IP) injection of 0.05 mg/g of buprenorphine analgesic. To induce mechanical overload of the plantaris (PLT) muscles, bilateral myotenectomy was performed by removing the distal tendon and myotendinous junction of the gastrocnemius muscle as previously described (62). Following the surgeries, incisions were closed with Vetbond surgical glue (Henry Schein, Melville, NY, USA). Control mice were subjected to a sham surgery where an incision was made on the lower leg and the wound similarly closed. Mice were allowed to recover for 7 d after which mice were re-anesthetized with isoflurane and the PLT muscles were collected, immediately frozen in liquid N_2, and subjected to Western blot analysis as described below.

Rapamycin injections

Rapamycin was purchased from LC laboratories (Woburn, MA, USA) and was dissolved in DMSO to generate a 5 µg/µl stock solution. The appropriate volume of the stock solution needed to inject mice at a dose of 1.5 mg/kg was dissolved in 200 µl of phosphate-buffered saline (PBS) and administered via an IP injection 2 h before the MTE or sham surgery (based on an average body mass of 20.9 ± 0.3 g for mice used in the MTE-induced overload experiments, the relative percentage of DMSO in each rapamycin, or vehicle, injection was 3.1%). Mice then received daily rapamycin IP injections for 7 d, with muscles being collected 24 h after the last injection.

Denervation-induced mechanical unloading

To examine the effect of denervation-induced muscle atrophy, unilateral denervation surgeries were performed under isoflurane anaesthesia by making a small incision in the skin and underlying musculature on the lateral proximal thigh parallel with the femur as previously described (23). The sciatic nerve was then isolated and a 3–4 mm section of the nerve cut out. Control mice were subjected to a sham surgery. Following the surgeries, incisions were closed with Vetbond surgical glue. Mice were allowed to recover for 7 d, after which the tibialis anterior (TA) muscle was collected under isoflurane anesthesia, frozen in liquid N_2, and subjected to Western blot analysis as described below.

Food Deprivation

To examine the effect of acute food deprivation (FD)-induced muscle atrophy, food was withheld from mice for 48 h, with *ad libitum* access to water, as previously described (27). Control mice were maintained on the *ad libitum* diet (AL). After 48 h, mice were anaesthetized with isoflurane and the TA muscles were collected, frozen in liquid N_2, and subjected to Western blot analysis as described below.

Puromycin injections and muscle collections for in vivo SUnSET measures of protein synthesis

To measure the relative differences in the rates of protein synthesis between treatments, we used our puromycin-based *in vivo* SUnSET method (26, 28). Puromycin was purchased from Millipore Sigma and was dissolved in water to generate a 75 mM stock solution. For all *in vivo* measurements of protein synthesis, 0.040 µmol/g body mass of puromycin in 100 µl of PBS was administered via an IP injection at 30 min before muscle collection (28). More specifically, 20 min after the puromycin injection, mice were anaesthetized with isoflurane and placed on a heated pad, the PLT or TA

muscles were exposed and then rapidly dissected at exactly 30 min post-puromycin injection and immediately frozen in liquid N_2.

Western Blotting

Frozen muscles were homogenized with an Omni homogenizer (Model #TH220) for 20 s in ice-cold buffer A [40 mM Tris (pH 7.5), 1 mM EDTA, 5 mM EGTA, 0.5% Triton X-100, 25 mM b-glycerophosphate, 25 mM NaF, 1 mM Na3VO4, 10 mg/ml leupeptin, and 1 mM PMSF]. The whole homogenate was used for further Western blot analysis. Sample protein concentration was determined with a DC protein assay kit (Bio-Rad, Hercules, CA, USA). Equivalent amounts of protein from each sample were dissolved in Laemmli buffer, heated to 100°C for 5 min, and then subjected to electrophoretic separation by SDS-PAGE. Following electrophoretic separation, proteins were transferred to a PVDF membrane and blocked with 5% powdered milk in TBS containing 0.1% Tween 20 (TBST) for 1 h followed by an overnight incubation at 4°C with primary antibody dissolved in TBST containing 1% bovine serum albumin. Primary antibodies used were: mouse anti-puromycin (mAB IgG2a 12D10, 1:5000, Millipore, #MABE343), rabbit anti-total $p70^{S6k1}$ (1:2000, CST, #9202), rabbit anti-$p70^{S6k1}$ T389 (1:1000, CST, #9205), rabbit anti-ornithine decarboxylase 1 (Odc1, 1:2000, ProteinTech, #17003-1-AP), rabbit anti-s-adenosylmethionine decarboxylase (Amd1, 1:250, Santa Cruz, #sc-1666970), rabbit anti-spermidine synthase (Srm, 1:1000, ProteinTech, #19858-1-AP), rabbit anti-spermine synthase (Sms, 1:1000, Abcam, #ab15147), rabbit anti-spermine oxidase (Smox, 1:1000, ProteinTech, #15052-1-AP), rabbit anti-spermidine/spermine N1-acetyltransferase 1 (Sat1, 1:1000, CST, #61586). After an overnight incubation, the membranes were washed for 30 min in TBST and then probed with a peroxidase conjugated secondary antibody for 1 h at room temperature. Secondary antibodies used were: anti-mouse IgG Fc 2a horseradish peroxidase-conjugated antibody (1:50,000, #115-035-206, Jackson ImmunoResearch Laboratories Inc., West Grove, PA, USA) and anti-rabbit IgG (H+L) horseradish peroxidase-conjugated antibody (1:5000, #PI-1000, Vector Laboratories, Burlingame, CA, USA). Following 30 min of washing in TBST, the blots were developed using ECL Prime reagent (Amersham, Piscataway, NJ, USA) and images were captured (Fusion FX imaging system, Vilber Lourmat, Germany). Densitometric analysis was performed using Fusion CAPT Advance software (Vilber Lourmat, Germany). Membranes were then stained for total protein with Coomassie Blue or Ponceau. The signal for the band of the protein of interest was then normalized to the signal for total protein in each lane.

Statistical analysis

Data are presented as Mean ± SEM, with all graphs displaying the results for individual samples. Statistical significance was determined by using a 2-way ANOVA, followed by a Tukey's post hoc analysis [for the 4 group myotenectomy (MTE) experiments], or a Student's unpaired, 2-tailed t-test [for the 2 group food deprivation (FD) and denervation (Den) experiments]. Differences between groups were considered significant when $p<0.05$. All statistical analyses were performed on GraphPad Prism v9 software.

Results

mTORC1 signalling, protein synthesis, skeletal muscle mass and polyamine pathway protein expression during mechanical overload-induced muscle hypertrophy.

To assess the regulation of polyamine pathway enzymes in response to mTORC1-mediated muscle growth, we subjected mice to bilateral myotenectomy (MTE) (62), or sham, surgeries and allowed mice to recover for 7 d with daily IP injections of the mTORC1 inhibitor, rapamycin, or vehicle control. First, to ensure that mTORC1 signalling would be inhibited prior to the mice recovering from the MTE or sham surgery and, therefore, prior to the initiation of overload on the plantaris (PLT) muscle, we injected mice with rapamycin (or vehicle) and collected PLT muscles 2 h later for Western blot analysis of the phosphorylation of the T389 residue of the direct mTORC1 substrate, $p70^{S6K1}$ (25, 30). As shown in Fig. 1A, the administration of rapamycin 2 h prior markedly inhibited mTORC1 signalling, demonstrating effective mTORC1 inhibition prior to the onset of mechanical overload.

Next, we examined changes in $p70^{S6K1}$ phosphorylation after 7 d of MTE-induced overload. As shown in Fig. 1B, $p70^{S6K1}$ T389 phosphorylation was elevated by 7 d of MTE-induced overload and this response was ablated by rapamycin treatment (Fig. 1B). Consistent with the increase in mTORC1 signalling, MTE induced a significant increase in muscle mass that was also inhibited by rapamycin (Fig. 1C). Having confirmed an adaptive increase in muscle mass associated with mechanical overload, we examined MTE-induced changes in the rate of protein synthesis using the puromycin-based SUnSET method and found that MTE induced an increase in the rate of protein synthesis, which was again inhibited by rapamycin (Fig. 1D). Combined, these data show MTE induced muscle hypertrophy that was associated with an increase in mTORC1 signalling and protein synthesis, and that these were all inhibited by rapamycin. Importantly, these data show that this model is appropriate to address the questions of whether polyamine pathway protein expression is altered during mechanical overload-induced muscle hypertrophy and whether mTORC1 may play a role.

To determine whether key components of the polyamine pathway were altered in muscles undergoing hypertrophy, we next examined the expression of one of first rate-limiting enzymes of

the polyamine pathway, Odc1. Unexpectedly, there was no significant effect of MTE or rapamycin on Odc1 protein (Fig. 2A). The second rate-limiting step of the polyamine pathway is catalysed by the enzyme, Amd1, and as shown in Fig. 2B, Amd1 was significantly upregulated by MTE and this response was largely inhibited by rapamycin. Similar to Amd1, the abundance of SpdSyn was also increased by MTE in a rapamycin-sensitive manner (Fig. 2C). In contrast, there was no effect of MTE or rapamycin on the abundance of SpmSyn, Smox or Sat1 proteins (Fig 2D-F). These data suggest that during chronic mechanical overload, Amd1 and SpdSyn protein abundance is regulated, in part, by rapamycin-sensitive, and presumably a mTORC1-dependent mechanism. mTORC1 is known to also positively regulate the translation of the mRNA encoding the transcription factor, c-Myc (8, 21, 59), and c-Myc is a positive regulator of Amd1 and SypSyn gene expression (17, 19). We have previously shown that c-Myc is markedly elevated by the more robust synergist ablation model of mechanical overload (24), however, whether c-Myc protein is upregulated by this milder MTE overload model is yet to be determined. As such, we also examined changes to c-Myc protein by MTE and found that, similar to Amd1 and SpdSyn, c-Myc was increased by MTE and this response was markedly inhibited by rapamycin (Fig. 2G). Overall, these data show that mechanical overload-induced muscle hypertrophy is associated with an increase in Amd1 and SpdSyn, suggesting a role for polyamine metabolism in this mechanical overload-based model of hypertrophic adaptation. Furthermore, these changes in Amd1 and SpdSyn are regulated by a rapamycin sensitive, and presumably mTORC1-dependent, manner that may involve c-Myc.

mTORC1 signalling, protein synthesis, skeletal muscle mass and polyamine pathway protein expression during muscle atrophy induced by food deprivation and denervation

Given the potential mTORC1-dependent changes in polyamine pathway proteins we observed during load-induced muscle hypertrophy, we hypothesised that key proteins of the polyamine pathway may also be altered in models of muscle atrophy. To address this question, we examined two models of atrophy that are characterised by two very different responses to mTORC1 signalling. Specifically, in the denervation (Den) model of muscle atrophy, mTORC1 is initially markedly elevated (23), while in the food deprivation (FD) model, mTORC1 signalling is markedly reduced (27). Firstly, we investigated the FD model and, as shown in Fig. 3, 48 h of FD resulted in the expected decreases in body mass (Fig. 3A), muscle mass (Fig. 3B), mTORC1 signalling (Fig. 3C) and protein synthesis (Fig. 3D) compared to the *ad libitum* (AL) fed controls. mTORC1 is also a negative regulator of autophagy and nutrient starvation is known to activate autophagy (45). As expected, FD led to an increase in the autophagy marker, LC3B-II, and the LC3B-II/LC3B-I ratio (Fig. 3E), indicating increased autophagy.

Regarding the polyamine pathway proteins, despite the decrease in mTORC1 signalling with FD, there was no change in the expression of Odc1, Amd1, SpdSyn, SpmSyn or Smox proteins with FD (Fig. 4A-E), nor a change in c-Myc protein (Fig. 4G). There was, however, a significant decrease in Sat1 (Fig. 4F). These data suggest a very limited effect on the expression of polyamine pathway proteins in muscles undergoing atrophy as a consequence of severe caloric restriction.

In the second model of muscle atrophy, 7 d of Den resulted in a significant decrease in muscle mass, with no change in body mass (data not shown), compared to muscles from sham control mice (Fig. 5A). In contrast to the FD model, Den-induced atrophy was associated with an increase in both LC3B-I and LC3B-II proteins, and a trend ($p = 0.07$) for an elevation in the LC3B-II/LC3B-I ratio (Fig. 5B). This difference in the expression of LC3B-I and LC3B-II between these two atrophy models may be related, in part, to the difference in mTORC1 activation with Den, which is likely to antagonise the induction, elongation and autophagosome maturation steps of autophagy [for review see (14)]. Indeed, as we, and others, have previously shown [e.g. (23, 55)], Den-induced atrophy was associated with a large increase in $p70^{S6K1}$ T389 phosphorylation, indicating increased mTORC1 signalling, and by a mild elevation in the rate of protein synthesis (Fig. 5C & D). Regarding polyamine pathway proteins, we found that Den was associated with a small decrease in Odc1 (Fig. 6A). Interestingly, similar to MTE-induced hypertrophy, Den was associated with increased SpdSyn and c-Myc (Fig. 6C & G); however, unlike MTE, Den did not result in a change in Amd1 (Fig. 6B). Instead, Den resulted in a marked increase in SpmSyn (Fig. 6D) and, unlike with FD-induced atrophy, Den was not associated with a change in Sat1 protein (Fig. 6F). These data suggest a positive correlation between mTORC1 signalling and the expression of c-Myc and SpdSyn proteins with Den, similar to that found with MTE-induced muscle hypertrophy, but not Amd1. Furthermore, unlike the FD model, Den-induced atrophy was associated with an increase in SpmSyn. Overall, these data suggest that the polyamine pathway is being differentially regulated in these models of muscle atrophy and this regulation of polyamines may play a role(s) in the respective adaptive responses.

Discussion

This is the first study to comprehensively investigate changes in the abundance of polyamine pathway enzymes in models of muscle hypertrophy and muscle atrophy. Overall, we find that specific proteins in this pathway are differentially regulated in the three different models, suggesting

317 that changes in the levels of specific polyamines and/or the rate of flux through the polyamine
318 pathway may play a role in the adaptation to these different imposed stressors.

319 A major aim of this study was to examine whether changes to polyamine pathway proteins might be
320 associated with the activation of mTORC1. To explore this hypothesis, we employed the MTE-
321 induced model of chronic mechanical overload that we have previously shown to induce muscle
322 hypertrophy in a rapamycin-sensitive and mTORC1-dependent manner (62). In this study, we again
323 confirm that MTE was sufficient to induce muscle hypertrophy and that this was associated with an
324 increase in mTORC1 signalling and protein synthesis. Furthermore, we showed that rapamycin
325 inhibited MTE-induced mTORC1 signalling, protein synthesis and muscle growth. Contrary to our
326 hypothesis, however, we did not find an increase in Odc1 protein, one of the rate-limiting enzymes
327 of the polyamine pathway. The regulation of Odc1 expression is, however, relatively complex,
328 including transcriptional, translational and post-translational mechanisms [for review see (46)]. For
329 example, in addition to transcriptional and translational regulation, Odc1 protein has one of the
330 shortest half-lives in mammalian cells [10-30 min (3)] that is mediated by a polyamine-induced
331 expression of the non-competitive inhibitor, antizyme (Az or Oaz), which forms a heterodimer with
332 Odc1, leading to ubiquitin-independent proteasome-mediated degradation (5, 6, 32). Furthermore,
333 another protein, antizyme inhibitor (Azin), has an even higher affinity for Az and, thus, competes
334 with Odc1 for binding to Az and inhibits Odc1 degradation (20, 33). While we did not detect an
335 increase in Odc1 at 7d after the initiation of mechanical overload, we cannot rule out that Odc1
336 levels may have been altered at an earlier time point. It has also been reported in non-muscle cells
337 that Odc1 is phosphorylated and that phosphorylation increases Odc1 activity (50) suggesting that
338 Odc1 activity could also be regulated independent of changes in Odc1 protein abundance. Clearly
339 future studies are required to investigate potential changes to Odc1 transcription, translation and/or
340 activity, and changes to Az and Azin expression, in this and other models of muscle growth.

341 Importantly, in contrast to Odc1, we found that MTE did induce an increase in the second rate-
342 limiting enzyme, Amd1. Furthermore, this overload-induced increase was markedly inhibited by
343 rapamycin, suggesting that the expression of Amd1 is regulated, in part, by a mTORC1-dependent
344 mechanism, and that Amd1 may play a role in the adaptation to chronic mechanical overload.
345 Similar to Odc1, Amd1 is regulated transcriptionally and translationally (17, 60), and also has a very
346 short half-life [~30 min; (54)]. One possible reason for increased Amd1 abundance is a
347 mTORC1/eIF4E-mediated increase in translational efficiency of the Amd1 mRNA that possess a long
348 and highly structured 5'-UTR (41, 53). In addition, the Amd1 gene has been shown to contain at least
349 one c-Myc-binding E-box upstream of the transcriptional start site (17). Our finding of an overload-
350 induced and rapamycin-sensitive increase in c-Myc protein suggests that mTORC1 could also have

contributed to the increase in Amd1 protein by facilitating an increase in c-Myc mRNA translation (8, 21, 59), leading to a c-Myc-mediated increase in Amd1 gene transcription (18). Another potential link between mTORC1 and Amd1 comes from a recent study that reported a high correlation between Amd1 levels and mTORC1 activity (i.e. $p70^{S6K1}$ phosphorylation) in prostate cancer cells (63). Subsequent analysis showed that Amd1 was a direct target of mTORC1 and that mutation of the mTORC1-mediated phosphorylated Amd1 residue (S298A) resulted in a reduced Amd1 protein half-life, suggesting that activated mTORC1 plays a post-translational role in increasing Amd1 stability (63). Unfortunately, there is currently no commercially available antibody to enable investigate of this potential mechanism in overloaded skeletal muscle. Nonetheless, these data strongly suggest a direct and/or indirect role for mTORC1 in regulating Amd1 expression during MTE-induced muscle hypertrophy. Interestingly, it has recently been shown that mTORC1, via c-Myc, also positively regulates the expression of the enzyme, MAT2A, which catalyzes the conversion of methionine to SAM (S-adenosylmethione), the product of one-carbon metabolism and the substrate for Amd1 (57). Furthermore, SAM is a known indirect activator of mTORC1 activity via binding to the protein, SAMTOR (31). These data suggest that, in addition to mTORC1 increasing the expression of the key polyamine pathway proteins, Amd1 and SpdSyn, mTORC1 may also increase SAM leading to enhanced mTORC1 activity and ensuring provision of Amd1 substrate for increased polyamine synthesis to support cell growth; however, this hypothesis is yet to be directly investigated in skeletal muscle.

Similar to Amd1, we found that SpdSyn was also upregulated by mechanical overload in a rapamycin-sensitive manner that again suggests the involvement of mTORC1. Possible reasons for the increase in SpdSyn protein also include mTORC1-mediated increases in translational efficiency of the highly structured SpdSyn mRNA (35, 41, 58) and/or an increase in c-Myc-mediated SpdSyn transcription, potentially facilitated by mTORC1 (8, 17, 19, 21, 59). Importantly, these findings suggest a role for Spd synthesis in the hypertrophic response to mechanical overload. These data are consistent with our previous finding that SpdSyn protein, but not mRNA, was upregulated at 2 and 28d after the induction of FST-induced muscle hypertrophy (10), and suggest a role for Spd synthesis in muscle growth more broadly. Interestingly, the overexpression of Smox, which converts Spm back to Spd, was recently shown to stimulate muscle fiber hypertrophy and inhibit various models of muscle fiber atrophy (2). Polyamines have been shown to play essential roles in facilitating protein turnover in cells, with the depletion of polyamines leading to a complete inhibition of protein synthesis and cell growth (40), an effect that is likely driven by depletion of Spd. For example, Spd is the precursor molecule required for the unique covalent post-translation modification, known as hypusination, of the translation factor, eIF5A [for review see (13)], and inhibition of eIF5A

hypusination leads to the ablation of protein synthesis in cultured muscle cells (12). Spermidine has also been shown to play an essential role in regulating autophagy (56), a process required for optimal protein turnover (51), in part, through its ability to inhibit histone, and autophagy-related protein, acetylation (16, 43, 48). When combined, the results from our MTE model suggest that Spd synthesis may play a critical role in the adaptive response to mechanical overload and that the up-regulation of SpdSyn expression, and subsequent increase in spermidine production, may be a fundamental component of the mTORC1-regulated network needed for the increase in protein turnover required for muscle hypertrophy. Figure 7 provides a graphical summary of the results from the MTE mechanical overload study, highlighting the role of mTORC1 in the activation of spermidine synthesis and its requirement for protein synthesis. Many questions, however, remain to be answered and further studies are needed to determine whether SpdSyn/Spd are, in fact, required for mechanically-induced increases in protein synthesis and muscle mass, and to determine the relative contributions of transcriptional and translational regulation of key polyamine pathway proteins in overload-induced muscle growth.

Another aim of this study was to determine whether the abundance of any of the major polyamine pathway enzymes would also be altered in models of muscle atrophy. The first model examined was 48 h food deprivation in which mTORC1 signalling and protein synthesis are markedly inhibited. In this model, we found no change in the proteins that were up regulated by MTE in a rapamycin-sensitive, and presumably a mTORC1-dependent manner (i.e. Amd1 or SpdSyn), suggesting that mTORC1 does not play a significant role in regulating the basal levels of these proteins under the condition of severe caloric restriction. The lack of change in Odc1 abundance was also an notable finding given that an early study has reported a marked (~80%) decrease in Odc1 activity in gastrocnemius/thigh muscle of rats starved for 48 h (7). Notwithstanding species and muscle differences between the two studies, these data suggest the possibility of post-translational regulation of Odc1 activity that is independent of protein abundance [e.g. phosphorylation (50)]. Recently, using the same antibody used in the current study, Bongers *et al* reported that Smox protein was down regulated after 24 h food deprivation in the TA muscles of male C57Bl/6 mice (2). This finding is in contrast to our observation of no change in Smox protein after 48 h of food deprivation in female FVB/N mice and raises the intriguing possibility of mouse strain or sex differences in regulation of Smox, or that Smox protein levels initially declined at 24 h but then recovered by 48 h. Finally, the one protein that we found to be altered by starvation was Sat1, which catalyses the rate-limiting step of Spd and Spm catabolism in a reaction that requires acetyl-CoA [for review see (47)]. Similar to other polyamine pathway proteins, the regulation of Sat1 expression is complex, with elevated polyamine levels increasing Sat1 transcription, mRNA stability and

translation, and decreasing proteasome-mediated protein degradation (47). As such, a decrease in muscle Sat1 protein with food deprivation would be consistent with decreased polyamine levels; however, further work is required to determine the exact mechanism(s) involved in regulating Sat1 expression in skeletal muscle and how this is related to polyamine levels under different conditions.

The second model of muscle atrophy examined in this study was denervation which, in contrast to food deprivation, is paradoxically characterised by elevated mTORC1 signalling (23, 55). Similar to the MTE hypertrophy model, the denervation-induced increase in mTORC1 signalling was again associated with increased SpdSyn and c-Myc; however, unlike MTE, there was no corresponding increase in Amd1. This lack of effect could suggest that Amd1 is, in fact, not regulated in a mTORC1-dependent manner, however, there is one other unique observation in this denervation model that may have an impact on this finding. Specifically, unlike with MTE, denervation was also associated with an increase in SpmSyn protein and Spm is known to be a potent inhibitor of Amd1 mRNA translation (53). The proposed mechanism involves a small open reading frame upstream (uORF) of the main Amd1 encoding reading frame which encodes for a small peptide (amino acid sequence: MAGDIS). In the presence of elevated Spm, this peptide causes ribosomes to stall during the termination step at this small uORF, therefore blocking access of ribosomes to the main Amd1 ORF and inhibiting Amd1 mRNA translation (37). Thus, despite the increase in mTORC1 signalling and SpdSyn protein abundance, denervation-induced atrophy may be associated with reduced levels of Spd due an increase in SpmSyn and a Spm-mediated inhibition of the upstream rate-limiting enzyme, Amd1. While this is an attractive hypothesis, significantly more work is required to elucidate the exact mechanism, including how SpmSyn expression is regulated.

Overall, the data from the FD and Den experimental models clearly demonstrates that the regulation of polyamine pathway proteins during muscle atrophy is not simply the reverse of what occurs during mechanically-induced muscle hypertrophy and is likely dependent on the type of atrophy stimulus. Nonetheless, these data again highlight the potential that the regulation of polyamine pathway enzymes/polyamines may play a critical role(s) in the remodelling of skeletal muscle in response to altered states of mechanical loading.

Limitations

In this study, we used three different models of skeletal muscle adaptation (one hypertrophic and 2 atrophic) to identify novel changes to proteins involved in polyamine metabolism. While these findings are important for our understanding of skeletal muscle plasticity, further loss-of function

and gain-of function studies are required to define the precise roles that polyamines play in the adaptive response to stress on muscle. Furthermore, while we chose to focus on changes at the protein level, a more comprehensive understanding of mechanisms that regulate the changes in these proteins (i.e. transcription vs translation vs protein degradation) will be obtained from also examining changes in mRNA expression and protein stability. Metabolomics and tracer studies are also required to measure changes in the concentrations of specific polyamine species in these models and to quantify fluxes through the pathway. Finally, time course studies will also be beneficial to investigate the temporal nature of the changes to polyamine pathway proteins and to individual polyamines.

Conclusion

This is the first study to examine changes to the major enzymes of the polyamine pathway in skeletal muscle using different physiological stressors. Our findings show that various polyamine pathway enzymes are differentially regulated in response to mechanical overload, starvation and denervation. Furthermore, we provide evidence that the expression of SpdSyn, Amd1 and c-Myc are regulated in a rapamycin-sensitive manner that supports a direct and/or indirect role for mTORC1 in the regulation of polyamines during overload-induced muscle hypertrophy. Furthermore, we show that while denervation-induced atrophy is also associated with an increase in mTORC1 signalling, SpdSyn and c-Myc, it is also associated with an increase in SpmSyn expression, which may ultimately inhibit Amd1 expression and suppress Spd synthesis. Overall, these novel data are consistent with a role for changes in polyamine levels and/or flux in the adaptive response of skeletal muscle and support the need for further research into polyamine metabolism in skeletal muscle.

References

1. **Bello-Fernandez C, Packham G, and Cleveland JL.** The ornithine decarboxylase gene is a transcriptional target of c-Myc. *Proceedings of the National Academy of Sciences of the United States of America* 90: 7804-7808, 1993.
2. **Bongers KS, Fox DK, Kunkel SD, Stebounova LV, Murry DJ, Pufall MA, Ebert SM, Dyle MC, Bullard SA, Dierdorff JM, and Adams CM.** Spermine oxidase maintains basal skeletal muscle gene expression and fiber size and is strongly repressed by conditions that cause skeletal muscle atrophy. *Am J Physiol Endocrinol Metab* 308: E144-158, 2015.
3. **Casero RA and Marton LJ.** Targeting polyamine metabolism and function in cancer and other hyperproliferative diseases. *Nat Rev Drug Discov* 6: 373-390, 2007.
4. **Casero RA, Murray Stewart T, and Pegg AE.** Polyamine metabolism and cancer: treatments, challenges and opportunities. *Nature Reviews Cancer* 18, 2018.
5. **Chen H, MacDonald A, and Coffino P.** Structural Elements of Antizymes 1 and 2 Are Required for Proteasomal Degradation of Ornithine Decarboxylase. *Journal of Biological Chemistry* 277: 45957-45961, 2002.
6. **Coffino P.** Regulation of cellular polyamines by antizyme. *Nature Reviews Molecular Cell Biology* 2: 188-194, 2001.
7. **Conover CA, Rozovski SJ, Belur ER, Aoki TT, and Ruderman NB.** Ornithine decarboxylase activity in insulin-deficient states. *The Biochemical journal* 192: 725-732, 1980.
8. **Csibi A, Lee G, Yoon S-O, Tong H, Ilter D, Elia I, Fendt S-M, Roberts Thomas M, and Blenis J.** The mTORC1/S6K1 Pathway Regulates Glutamine Metabolism through the eIF4B-Dependent Control of c-Myc Translation. *Current Biology* 24: 2274-2280, 2014.
9. **Dai N, Rapley J, Angel M, Yanik MF, Blower MD, and Avruch J.** mTOR phosphorylates IMP2 to promote IGF2 mRNA translation by internal ribosomal entry. *Genes & Development* 25: 1159-1172, 2011.
10. **Davey JR, Watt KI, Parker BL, Chaudhuri R, Ryall JG, Cunningham L, Qian H, Sartorelli V, Sandri M, Chamberlain J, James DE, and Gregorevic P.** Integrated expression analysis of muscle hypertrophy identifies Asb2 as a negative regulator of muscle mass. *JCI Insight* 1, 2016.
11. **De Benedetti A and Graff JR.** eIF-4E expression and its role in malignancies and metastases. *Oncogene* 23: 3189-3199, 2004.
12. **de Proença ARG, Pereira KD, Meneguello L, Tamborlin L, and Luchessi AD.** Insulin action on protein synthesis and its association with eIF5A expression and hypusination. *Molecular Biology Reports* 46: 587–596, 2018.
13. **Dever TE, Gutierrez E, and Shin B-S.** The hypusine-containing translation factor eIF5A. *Critical Reviews in Biochemistry and Molecular Biology* 49: 413-425, 2014.
14. **Dossou AS and Basu A.** The Emerging Roles of mTORC1 in Macromanaging Autophagy. *Cancers* 11: 1422, 2019.
15. **Dubois V, Simitsidellis I, Laurent MR, Jardi F, Saunders PTK, Vanderschueren D, and Claessens F.** Enobosarm (GTx-024) Modulates Adult Skeletal Muscle Mass Independently of the Androgen Receptor in the Satellite Cell Lineage. *Endocrinology* 156: 4522-4533, 2015.
16. **Eisenberg T, Knauer H, Schauer A, Büttner S, Ruckenstuhl C, Carmona-Gutierrez D, Ring J, Schroeder S, Magnes C, Antonacci L, Fussi H, Deszcz L, Hartl R, Schraml E, Criollo A, Megalou E, Weiskopf D, Laun P, Heeren G, Breitenbach M, Grubeck-Loebenstein B, Herker E, Fahrenkrog B, Fröhlich K-U, Sinner F, Tavernarakis N, Minois N, Kroemer G, and Madeo F.** Induction of autophagy by spermidine promotes longevity. *Nature Cell Biology* 11: 1305-1314, 2009.
17. **Fernandez PC, Frank SR, Wang L, Schroeder M, Liu S, Greene J, Cocito A, and Amati B.** Genomic targets of the human c-Myc protein. *Genes Dev* 17: 1115-1129, 2003.
18. **Flynn A and Hogarty M.** Myc, Oncogenic Protein Translation, and the Role of Polyamines. *Medical Sciences* 6, 2018.
19. **Forshell TP, Rimpi S, and Nilsson JA.** Chemoprevention of B-cell lymphomas by inhibition of the Myc target spermidine synthase. *Cancer Prev Res (Phila)* 3: 140-147, 2010.

20. **Fujita K, Murakami Y, and Hayashi S.** A macromolecular inhibitor of the antizyme to ornithine decarboxylase. *The Biochemical journal* 204: 647-652, 1982.
21. **Gera JF, Mellinghoff IK, Shi Y, Rettig MB, Tran C, Hsu J-h, Sawyers CL, and Lichtenstein AK.** AKT Activity Determines Sensitivity to Mammalian Target of Rapamycin (mTOR) Inhibitors by Regulating Cyclin D1 and c-myc Expression. *Journal of Biological Chemistry* 279: 2737-2746, 2004.
22. **Goodman CA.** The Role of mTORC1 in Mechanically-Induced Increases in Translation and Skeletal Muscle Mass. *Journal of Applied Physiology* 127: 581-590, 2019.
23. **Goodman CA, Coenen AM, Frey JW, You J-S, Barker RG, Frankish BP, Murphy RM, and Hornberger TA.** Insights into the role and regulation of TCTP in skeletal muscle. *Oncotarget* 8: 18754-18772, 2017.
24. **Goodman CA, Dietz JM, Jacobs BL, McNally RM, You J-S, and Hornberger TA.** Yes-Associated Protein is up-regulated by mechanical overload and is sufficient to induce skeletal muscle hypertrophy. *FEBS letters* 589: 1491-1497, 2015.
25. **Goodman CA, Frey JW, Mabrey DM, Jacobs BL, Lincoln HC, You J-S, and Hornberger TA.** The role of skeletal muscle mTOR in the regulation of mechanical load-induced growth. *J Physiol* 589: 5485-5501, 2011.
26. **Goodman CA and Hornberger TA.** Measuring protein synthesis with SUnSET: a valid alternative to traditional techniques? *Exercise and sport sciences reviews* 41: 107-115, 2013.
27. **Goodman CA, Kotecki JA, Jacobs BL, and Hornberger TA.** Muscle Fiber Type-Dependent Differences in the Regulation of Protein Synthesis. *PLoS ONE* 7: e37890, 2012.
28. **Goodman CA, Mabrey DM, Frey JW, Miu MH, Schmidt EK, Pierre P, and Hornberger TA.** Novel insights into the regulation of skeletal muscle protein synthesis as revealed by a new nonradioactive in vivo technique. *FASEB J* 25: 1028-1039, 2011.
29. **Goodman CA, Mayhew DL, and Hornberger TA.** Recent Progress towards Understanding the Molecular Mechanisms that Regulate Skeletal Muscle Mass. *Cellular signalling 23*: 1896-1906, 2011.
30. **Goodman CA, Miu MH, Frey JW, Mabrey DM, Lincoln HC, Ge Y, Chen J, and Hornberger TA.** A Phosphatidylinositol 3-Kinase/Protein Kinase B-independent Activation of Mammalian Target of Rapamycin Signaling Is Sufficient to Induce Skeletal Muscle Hypertrophy. *Mol Biol Cell* 21: 3258-3268, 2010.
31. **Gu X, Orozco JM, Saxton RA, Condon KJ, Liu GY, Krawczyk PA, Scaria SM, Harper JW, Gygi SP, and Sabatini DM.** SAMTOR is an S-adenosylmethionine sensor for the mTORC1 pathway. *Science (New York, NY* 358: 813, 2017.
32. **Heller JS, Fong WF, and Canellakis ES.** Induction of a protein inhibitor to ornithine decarboxylase by the end products of its reaction. *Proceedings of the National Academy of Sciences of the United States of America* 73: 1858-1862, 1976.
33. **Kahana C.** Antizyme and antizyme inhibitor, a regulatory tango. *Cellular and Molecular Life Sciences* 66: 2479-2488, 2009.
34. **Kang SA, Pacold ME, Cervantes CL, Lim D, Lou HJ, Ottina K, Gray NS, Turk BE, Yaffe MB, and Sabatini DM.** mTORC1 Phosphorylation Sites Encode Their Sensitivity to Starvation and Rapamycin. *Science (New York, NY* 341, 2013.
35. **Kauppinen L.** Regulation of the human spermidine synthase mRNA translation by its 5'-untranslated region. *FEBS letters* 365: 61-65, 1995.
36. **Kemaladewi DU, Benjamin JS, Hyatt E, Ivakine EA, and Cohn RD.** Increased polyamines as protective disease modifiers in Congenital Muscular Dystrophy. *Human Molecular Genetics* 11: 1905–1912, 2018.
37. **Law GL, Raney A, Heusner C, and Morris DR.** Polyamine regulation of ribosome pausing at the upstream open reading frame of S-adenosylmethionine decarboxylase. *Journal of Biological Chemistry* 276: 38036–38043, 2001.
38. **Lee NKL, Skinner JPJ, Zajac JD, and MacLean HE.** Ornithine decarboxylase is upregulated by the androgen receptor in skeletal muscle and regulates myoblast proliferation. *American Journal of Physiology - Endocrinology And Metabolism* 301: E172-E179, 2011.

39. **MacLean HE, Chiu WSM, Notini AJ, Axell A-M, Davey RA, McManus JF, Ma C, Plant DR, Lynch GS, and Zajac JD.** Impaired skeletal muscle development and function in male, but not female, genomic androgen receptor knockout mice. *The FASEB Journal* 22: 2676-2689, 2008.

40. **Mandal S, Mandal A, Johansson HE, Orjalo AV, and Park MH.** Depletion of cellular polyamines, spermidine and spermine, causes a total arrest in translation and growth in mammalian cells. *Proceedings of the National Academy of Sciences of the United States of America* 110: 2169-2174, 2013.

41. **Manzella JM, Rychlik W, Rhoads RE, Hershey JW, and Blackshear PJ.** Insulin induction of ornithine decarboxylase. Importance of mRNA secondary structure and phosphorylation of eucaryotic initiation factors eIF-4B and eIF-4E. *Journal of Biological Chemistry* 266: 2383-2389, 1991.

42. **Meyuhas O and Dreazen A.** Ribosomal Protein S6 Kinase From TOP mRNAs to Cell Size. *Prog Mol Biol Transl Sci* 90C: 109-153, 2009.

43. **Morselli E, Mariño G, Bennetzen MV, Eisenberg T, Megalou E, Schroeder S, Cabrera S, Bénit P, Rustin P, Criollo A, Kepp O, Galluzzi L, Shen S, Malik SA, Maiuri MC, Horio Y, López-Otín C, Andersen JS, Tavernarakis N, Madeo F, and Kroemer G.** Spermidine and resveratrol induce autophagy by distinct pathways converging on the acetylproteome. *The Journal of cell biology* 192: 615, 2011.

44. **Mossmann D, Park S, and Hall MN.** mTOR signalling and cellular metabolism are mutual determinants in cancer. *Nature Reviews Cancer*, 2018.

45. **Noda T.** Regulation of Autophagy through TORC1 and mTORC1. *Biomolecules* 7, 2017.

46. **Pegg AE.** Regulation of Ornithine Decarboxylase. *Journal of Biological Chemistry* 281: 14529-14532, 2006.

47. **Pegg AE.** Spermidine/spermine-N1-acetyltransferase: a key metabolic regulator. *American Journal of Physiology-Endocrinology and Metabolism* 294: E995-E1010, 2008.

48. **Pietrocola F, Lachkar S, Enot DP, Niso-Santano M, Bravo-San Pedro JM, Sica V, Izzo V, Maiuri MC, Madeo F, Mariño G, and Kroemer G.** Spermidine induces autophagy by inhibiting the acetyltransferase EP300. *Cell Death And Differentiation* 22: 509-516, 2015.

49. **Ponnusamy S, Sullivan RD, You D, Zafar N, He Yang C, Thiyagarajan T, Johnson DL, Barrett ML, Koehler NJ, Star M, Stephenson EJ, Bridges D, Cormier SA, Pfeffer LM, and Narayanan R.** Androgen receptor agonists increase lean mass, improve cardiopulmonary functions and extend survival in preclinical models of Duchenne muscular dystrophy. *Human Molecular Genetics* 26: 2526-2540, 2017.

50. **Reddy SG, Mcllheran SM, Cochran BJ, Worth LL, Bishop LA, Brown PJ, Knutson VP, and Haddox MK.** Multisite Phosphorylation of Ornithine Decarboxylase in Transformed Macrophages Results in Increased Intracellular Enzyme Stability and Catalytic Efficiency. *Journal of Biological Chemistry* 271: 24945-24953, 1996.

51. **Sawan SA, Mazzulla M, Moore DR, and Hodson N.** More than just a garbage can: emerging roles of the lysosome as an anabolic organelle in skeletal muscle. *American Journal of Physiology-Cell Physiology* 319: C561-C568, 2020.

52. **Seidel ER and Ragan VL.** Inhibition by rapamycin of ornithine decarboxylase and epithelial cell proliferation in intestinal IEC-6 cells in culture. *British journal of pharmacology* 120: 571-574, 1997.

53. **Shantz LM, Viswanath R, and Pegg AE.** Role of the 5'-untranslated region of mRNA in the synthesis of S-adenosylmethionine decarboxylase and its regulation by spermine. *The Biochemical journal* 302 (Pt 3): 765-772, 1994.

54. **Shirahata A and Pegg AE.** Regulation of S-adenosylmethionine decarboxylase activity in rat liver and prostate. *Journal of Biological Chemistry* 260: 9583-9588, 1985.

55. **Tang H, Inoki K, Lee M, Wright E, Khuong A, Sugiarto S, Garner M, Paik J, Depinho RA, Goldman D, Guan KL, and Shrager JB.** mTORC1 Promotes Denervation-Induced Muscle Atrophy Through a Mechanism Involving the Activation of FoxO and E3 Ubiquitin Ligases. *Sci Signal* 7: ra18, 2014.

56. **Vanrell MC, Cueto JA, Barclay JJ, Carrillo C, Colombo MI, Gottlieb RA, and Romano PS.** Polyamine depletion inhibits the autophagic response modulating Trypanosoma cruzi infectivity. *Autophagy* 9: 1080-1093, 2013.

57. **Villa E, Sahu U, O'Hara BP, Ali ES, Helmin KA, Asara JM, Gao P, Singer BD, and Ben-Sahra I.** mTORC1 stimulates cell growth through SAM synthesis and m6A mRNA-dependent control of protein synthesis. *Molecular Cell*, 2021.

58. **Wahlfors J, Alhonen L, Kauppinen L, Hyvonen T, Janne J, and Eloranta TO.** Human spermidine synthase: cloning and primary structure. *DNA and cell biology* 9: 103-110, 1990.

59. **Wall M, Poortinga G, Hannan KM, Pearson RB, Hannan RD, and McArthur GA.** Translational control of c-MYC by rapamycin promotes terminal myeloid differentiation. *Blood* 112: 2305-2317, 2008.

60. **White MW, Degnin C, Hill J, and Morris DR.** Specific regulation by endogenous polyamines of translational initiation of S-adenosylmethionine decarboxylase mRNA in Swiss 3T3 fibroblasts. *The Biochemical journal* 268: 657-660, 1990.

61. **Winbanks CE, Weeks KL, Thomson RE, Sepulveda PV, Beyer C, Qian H, Chen JL, Allen JM, Lancaster GI, Febbraio MA, Harrison CA, McMullen JR, Chamberlain JS, and Gregorevic P.** Follistatin-mediated skeletal muscle hypertrophy is regulated by Smad3 and mTOR independently of myostatin. *The Journal of cell biology* 197: 997-1008, 2012.

62. **You J-S, McNally RM, Jacobs BL, Privett RE, Gundermann DM, Lin K-H, Steinert ND, Goodman CA, and Hornberger TA.** The role of raptor in the mechanical load-induced regulation of mTOR signaling, protein synthesis, and skeletal muscle hypertrophy. *FASEB J* 33: 4021-4034, 2019.

63. **Zabala-Letona A, Arruabarrena-Aristorena A, Martín-Martín N, Fernandez-Ruiz S, Sutherland JD, Clasquin M, Tomas-Cortazar J, Jimenez J, Torres I, Quang P, Ximenez-Embun P, Bago R, Ugalde-Olano A, Loizaga-Iriarte A, Lacasa-Viscasillas I, Unda M, Torrano V, Cabrera D, van Liempd SM, Cendon Y, Castro E, Murray S, Revandkar A, Alimonti A, Zhang Y, Barnett A, Lein G, Pirman D, Cortazar AR, Arreal L, Prudkin L, Astobiza I, Valcarcel-Jimenez L, Zuñiga-García P, Fernandez-Dominguez I, Piva M, Caro-Maldonado A, Sánchez-Mosquera P, Castillo-Martín M, Serra V, Beraza N, Gentilella A, Thomas G, Azkargorta M, Elortza F, Farràs R, Olmos D, Efeyan A, Anguita J, Muñoz J, Falcón-Pérez JM, Barrio R, Macarulla T, Mato JM, Martinez-Chantar ML, Cordon-Cardo C, Aransay AM, Marks K, Baselga J, Tabernero J, Nuciforo P, Manning BD, Marjon K, and Carracedo A.** mTORC1-dependent AMD1 regulation sustains polyamine metabolism in prostate cancer. *Nature* 554: 554, 2017.

Figure Legends

Figure 1: Mechanical overload-induced increases in mTORC1 signalling, muscle mass and protein synthesis. Mice were injected with rapamycin (Rap or R; 1.5 mg/kg) or vehicle (Veh or V), 2 h prior to undergoing myotenectomy (MTE), or sham (Sham), surgery. Mice were then subjected to daily IP injections of Rap or Veh for 7 d after which plantaris muscles were collected 30 min after an IP injection of puromycin (see Methods). **A.** The effect of a single rapamycin dose on $p70^{S6K1}$ T389 phosphorylation relative to total $p70^{S6K1}$ (P-$p70^{S6K1T389}$ /Total $p70^{S6K1}$ Ratio) 2 h prior to MTE or Sham surgery. **B-D:** The effect of 7 d MTE-induced overload, with and without daily rapamycin IP injections, on the P-$p70^{S6K1T389}$ /Total $p70^{S6K1}$ Ratio (**B**), plantaris muscle mass relative to body mass (**C**), and the rate of protein synthesis as assessed by the abundance of puromycin-labelled peptides (**D**). With the exception of muscle mass, all other values are expressed relative to Vehicle or Vehicle Sham controls. Data are Mean ± SEM (n = 3-4/group). # Significantly different from Vehicle treated groups. * Significantly different from all other groups, $p < 0.05$. Unpaired, two-tailed t-test or Two-way ANOVA with Tukey's post-test.

Figure 2: The effect of mechanical overload on polyamine pathway proteins. Mice were injected with rapamycin (Rap or R; 1.5 mg/kg) or vehicle (Veh or V), 2 h prior to undergoing myotenectomy (MTE), or sham, surgery. Mice were then subjected to daily IP injections of Rap or Veh for 7 d after which plantaris muscles were collected. Muscles were subjected to Western blot analysis for polyamine pathway-associated proteins: Ornithine decarboxylase 1 (Odc1. **A**). Adenosylmethionine decarboxylase 1 (Amd1, **B**), Spermidine synthase (SpdSyn, **C**), Spermine Synthase (SpmSyn, **D**), Spermine oxidase (Smox, **E**), Spermidine/spermine acetyltransferase 1 (Sat1, **F**) and c-Myc (**G**). Data are Mean ± SEM (n = 3-4/group). *Significantly different from all other groups, $p < 0.05$. Two-way ANOVA with Tukey's post-test.

Figure 3: Food deprivation-induced changes in body mass, muscle mass, mTORC1 signalling, protein synthesis and autophagy markers. Mice were allowed *ad libitum* (AL) access to food or were food deprived (FD) for 48 h. Thirty min prior to dissection of the tibialis anterior (TA) muscle, mice were given an IP injection of puromycin (see Methods). TA muscles were subjected to Western blot analysis. **A-E:** The effect of FD on body mass (**A**), muscle mass (**B**), $p70^{S6K1}$ T389 phosphorylation relative to total $p70^{S6K1}$ (P-$p70^{S6K1T389}$ /Total $p70^{S6K1}$ Ratio) (**C**), protein synthesis as assessed by the abundance of puromycin-labelled peptides (**D**) and the autophagy markers LC3B-I, LC3B-II and the LC3B-I/II ratio (**E**). With the exception of body mass and muscle mass, all other values are expressed

relative to AL controls. Data are Mean ± SEM (n = 4/group). * Significantly different from AL group, p < 0.05. Unpaired, two-tailed t-tests.

Figure 4: The effect of food deprivation on polyamine pathway proteins. Mice allowed *ad libitum* (AL) access to food or were food deprived (FD) for 48 h. Tibialis anterior muscles were subjected to Western blot analysis for polyamine pathway-associated proteins: Ornithine decarboxylase 1 (Odc1. **A**). Adenosylmethionine decarboxylase 1 (Amd1, **B**), Spermidine synthase (SpdSyn, **C**), Spermine Synthase (SpmSyn, **D**), Spermine oxidase (Smox, **E**), Spermidine/spermine acetyltransferase 1 (Sat1, **F**) and c-Myc (**G**). Data are Mean ± SEM, n = 4/group. All values are expressed relative to Sham controls. * Significantly different from AL group, p < 0.05. Unpaired, two-tailed, t-test.

Figure 5: Denervation-induced changes in muscle mass, autophagy markers, mTORC1 signalling and protein synthesis. Mice were subjected to sciatic nerve denervation (Den), or sham (Sham), surgery and allowed to recover for 7 d. Thirty min prior to dissection of the tibialis anterior (TA) muscle, mice were given an IP injection of puromycin (see Methods). TA muscles were subjected to Western blot analysis. **A-E:** The effect of Den on muscle mass to body mass ratio (**A**), the autophagy markers LC3B-I, LC3B-II and the LC3B-I/II ratio (**B**), $p70^{S6K1}$ T389 phosphorylation relative to total $p70^{S6K1}$ ($P\text{-}p70^{S6K1T389}$ /Total $p70^{S6K1}$ Ratio) (**C**), protein synthesis as assessed by the abundance of puromycin-labelled peptides (**D**). With the exception of muscle mass, all other values are expressed relative to Sham controls. Data are Mean ± SEM (n = 3-4/group). * Significantly different from Sham group, p < 0.05. Unpaired, two-tailed t-tests.

Figure 6: The effect of denervation on polyamine pathway proteins. Mice were subjected to unilateral sciatic nerve denervation (Den), or sham (Sham), surgery and allowed to recover for 7 d. Tibialis anterior muscles were subjected to Western blot analysis for polyamine pathway-associated proteins: Ornithine decarboxylase 1 (Odc1. **A**). Adenosylmethionine decarboxylase 1 (Amd1, **B**), Spermidine synthase (SpdSyn, **C**), Spermine Synthase (SpmSyn, **D**), Spermine oxidase (Smox, **E**), Spermidine/spermine acetyltransferase 1 (Sat1, **F**) and c-Myc (**G**). Mean ± SEM, n = 4/group. All values are expressed relative to Sham controls. * Significantly different from Sham, p < 0.05. Unpaired, two-tailed, t-test.

Figure 7: A summary of the potential role of mTORC1 in regulating the polyamine pathway during mechanical overload to support increases in protein synthesis and muscle hypertrophy. The results to the myotenectomy (MTE) study suggest that the mechanical activation of mTORC1 leads to

rapamycin-sensitive increase in Amd1 and SpdSyn proteins, possibly via increased Amd1 and SypSyn mRNA translation and/or via a c-Myc-mediated increase in Amd1 and SpdSyn transcription. Combined, these may lead to an increase in spermidine synthesis which is required for the hypusination of eIF5A which, in turn, is required for protein synthesis. Solid arrows indicate direct interactions or reactions. Dotted lines indicate multi-step processes. Definition of abbreviations: Odc1, ornithine decarboxylase 1; Amd1, adenosylmethionine decarboxylase 1; SpdSyn, spermidine synthase; SpmSyn, spermine synthase; Smox, spermine oxidase; Sat1, spermidine/spermine acetyltransferase 1; SAM, S-adenosylmethionine; dcSAM, decarboxylated SAM; MAT2A, Methionine Adenosyltransferase 2A ; MTA, 5-methylthioadenosine; hyp-eIF5A, hypusinated eukaryotic initiation factor 5A; mTORC1, mechanistic target of rapamycin; SAMTOR, S-adenosylmethionine sensor upstream of mTORC1. This figure was created using BioRender.

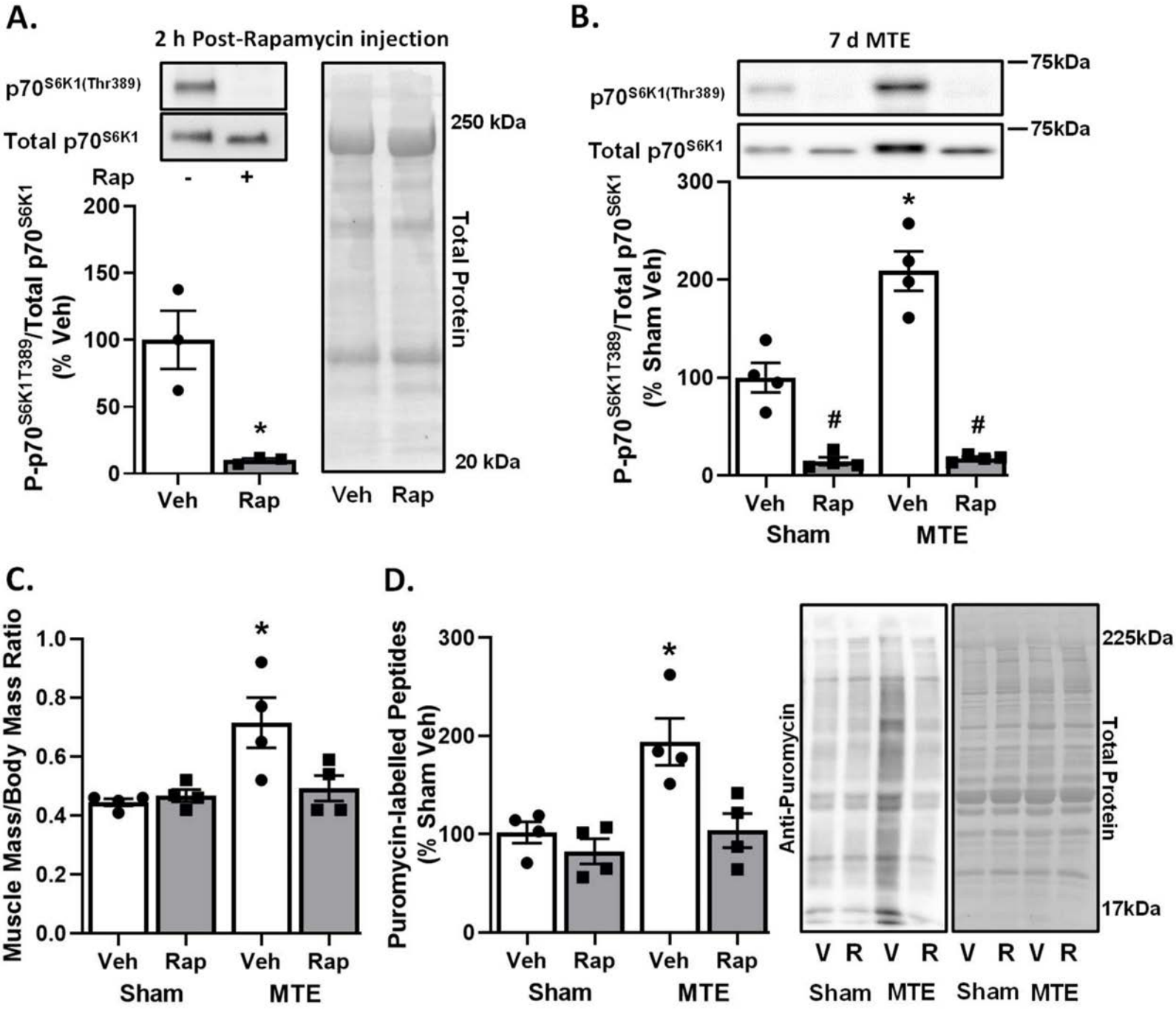
A.
2 h Post-Rapamycin injection
p70S6K1(Thr389)
Total p70S6K1
Rap - +
250 kDa
Total Protein
20 kDa
P-p70S6K1T389/Total p70S6K1 (% Veh)
200
150
100
50
0
*
Veh Rap Veh Rap
B.
7 d MTE
75kDa
75kDa
p70S6K1(Thr389)
Total p70S6K1
P-p70S6K1T389/Total p70S6K1 (% Sham Veh)
300
200
100
0
*
#
#
Veh Rap Veh Rap
Sham MTE
C.
Muscle Mass/Body Mass Ratio
1.0
0.8
0.6
0.4
0.2
0.0
*
Veh Rap Veh Rap
Sham MTE
D.
Puromycin-labelled Peptides (% Sham Veh)
300
200
100
0
*
Veh Rap Veh Rap
Sham MTE
Anti-Puromycin
225kDa
Total Protein
17kDa
V R V R V R V R
Sham MTE Sham MTE

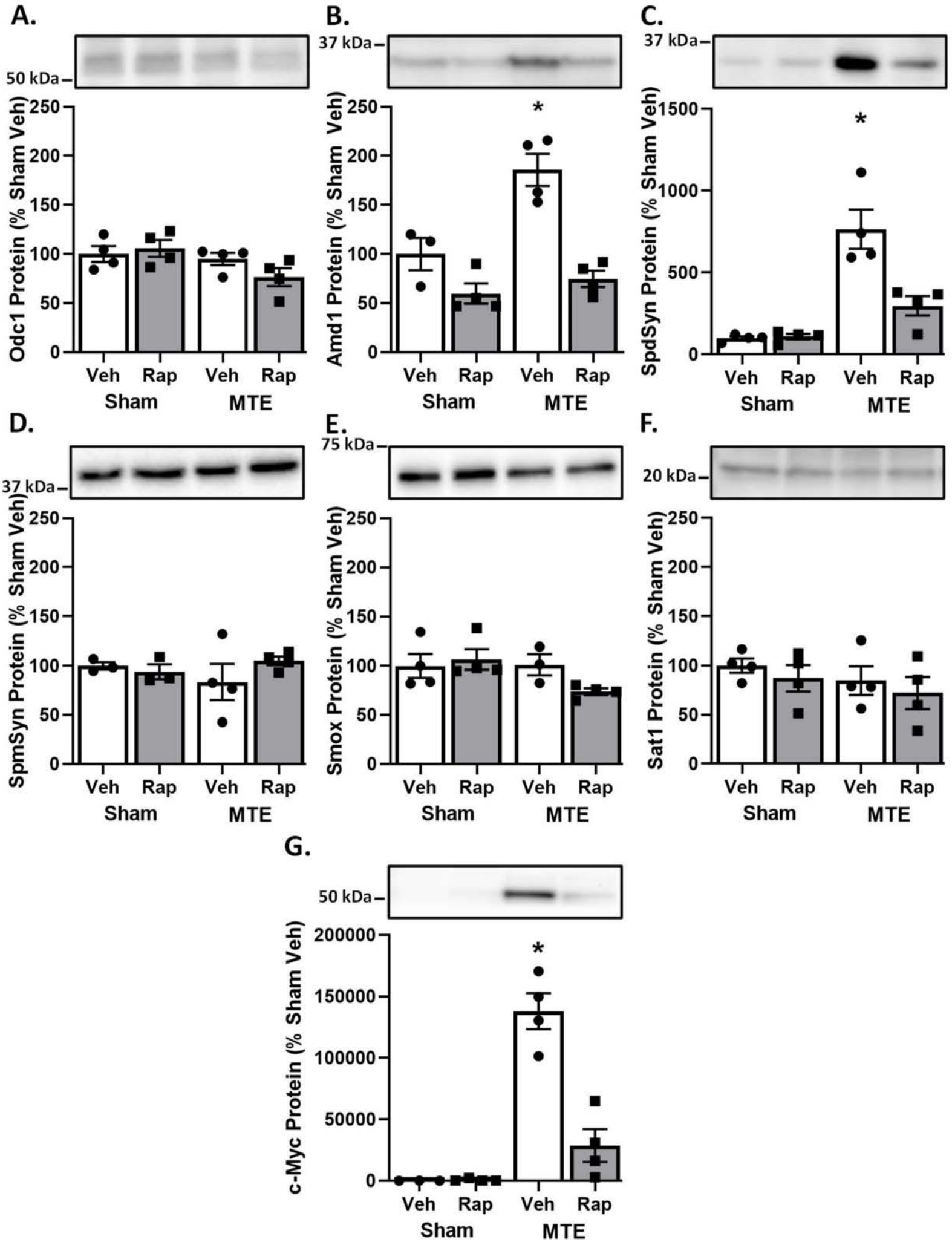
A.
50 kDa
Odc1 Protein (% Sham Veh)
250
200
150
100
50
0
Veh
Rap
Veh
Rap
Sham
MTE
B.
37 kDa
Amd1 Protein (% Sham Veh)
*
C.
37 kDa
SpdSyn Protein (% Sham Veh)
1500
1000
500
*
D.
37 kDa
SpmSyn Protein (% Sham Veh)
E.
75 kDa
Smox Protein (% Sham Veh)
F.
20 kDa
Sat1 Protein (% Sham Veh)
G.
50 kDa
c-Myc Protein (% Sham Veh)
200000
150000
100000
50000
0
*

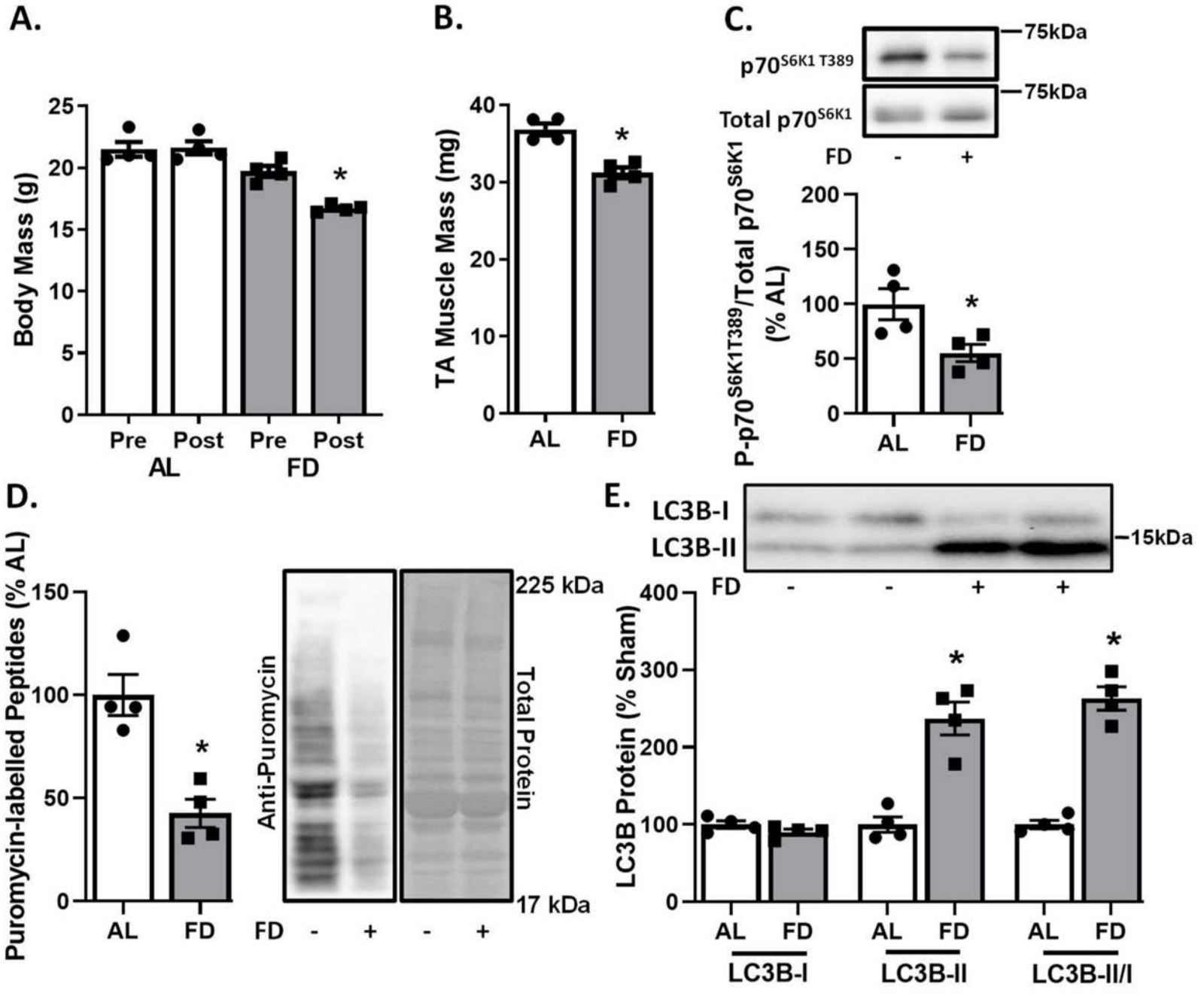
A.
Body Mass (g)
25
20
15
10
5
0
Pre
Post
Pre
Post
AL
FD
*
B.
TA Muscle Mass (mg)
40
30
20
10
0
AL
FD
*
C.
p70S6K1 T389
Total p70S6K1
75kDa
75kDa
FD - +
P-p70S6K1T389/Total p70S6K1 (% AL)
200
150
100
50
0
AL
FD
*
D.
Puromycin-labelled Peptides (% AL)
150
100
50
0
AL
FD
*
Anti-Puromycin
Total Protein
225 kDa
17 kDa
FD - + - +
E.
LC3B-I
LC3B-II
15kDa
FD - - + +
LC3B Protein (% Sham)
400
300
200
100
0
*
*
AL
FD
AL
FD
AL
FD
LC3B-I
LC3B-II
LC3B-II/I

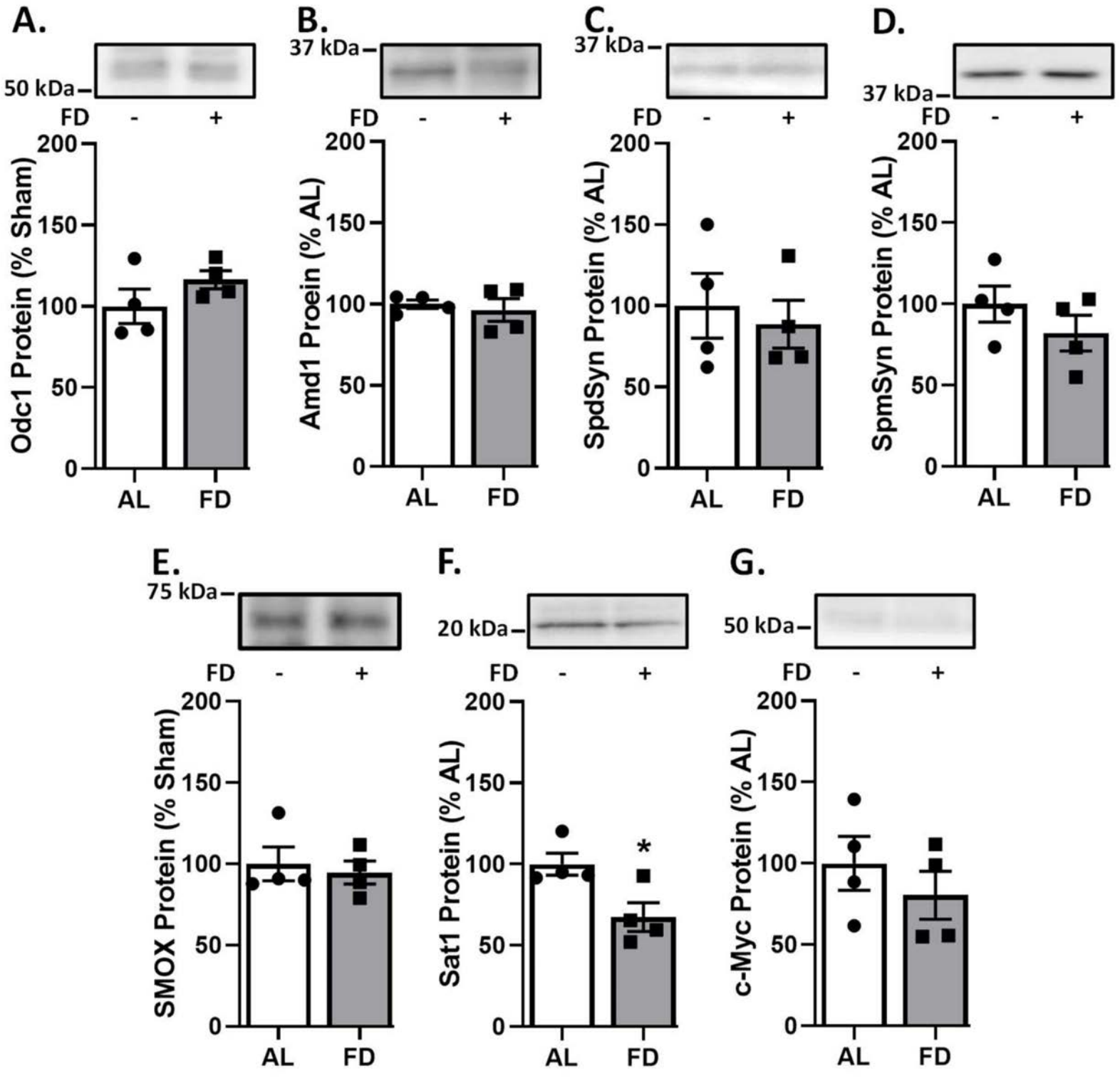
A.
50 kDa
FD - +
Odc1 Protein (% Sham)
200
150
100
50
0
AL FD
B.
37 kDa
FD - +
Amd1 Proein (% AL)
200
150
100
50
0
AL FD
C.
37 kDa
FD - +
SpdSyn Protein (% AL)
200
150
100
50
0
AL FD
D.
37 kDa
FD - +
SpmSyn Protein (% AL)
200
150
100
50
0
AL FD
E.
75 kDa
FD - +
SMOX Protein (% Sham)
200
150
100
50
0
AL FD
F.
20 kDa
FD - +
Sat1 Protein (% AL)
*
200
150
100
50
0
AL FD
G.
50 kDa
FD - +
c-Myc Protein (% AL)
200
150
100
50
0
AL FD

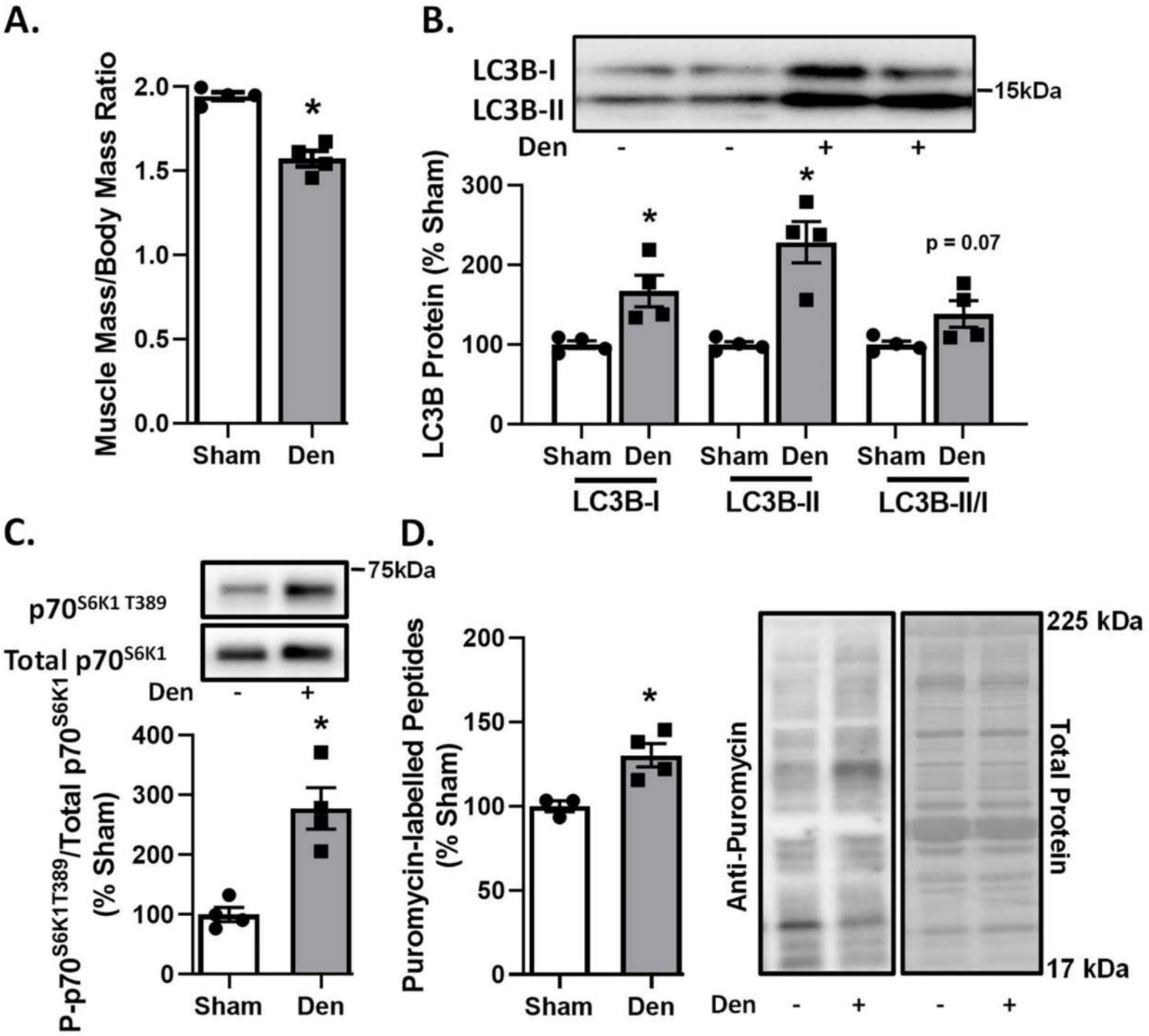
A.
Muscle Mass/Body Mass Ratio
2.0
1.5
1.0
0.5
0.0
*
Sham
Den
B.
LC3B-I
LC3B-II
15kDa
Den - - + +
LC3B Protein (% Sham)
300
200
100
0
*
*
p = 0.07
Sham Den Sham Den Sham Den
LC3B-I
LC3B-II
LC3B-II/I
C.
75kDa
p70S6K1 T389
Total p70S6K1
Den - +
P-p70S6K1T389/Total p70S6K1 (% Sham)
400
300
200
100
0
*
Sham
Den
D.
Puromycin-labelled Peptides (% Sham)
200
150
100
50
0
*
Sham
Den
Anti-Puromycin
Total Protein
225 kDa
17 kDa
Den - + - +

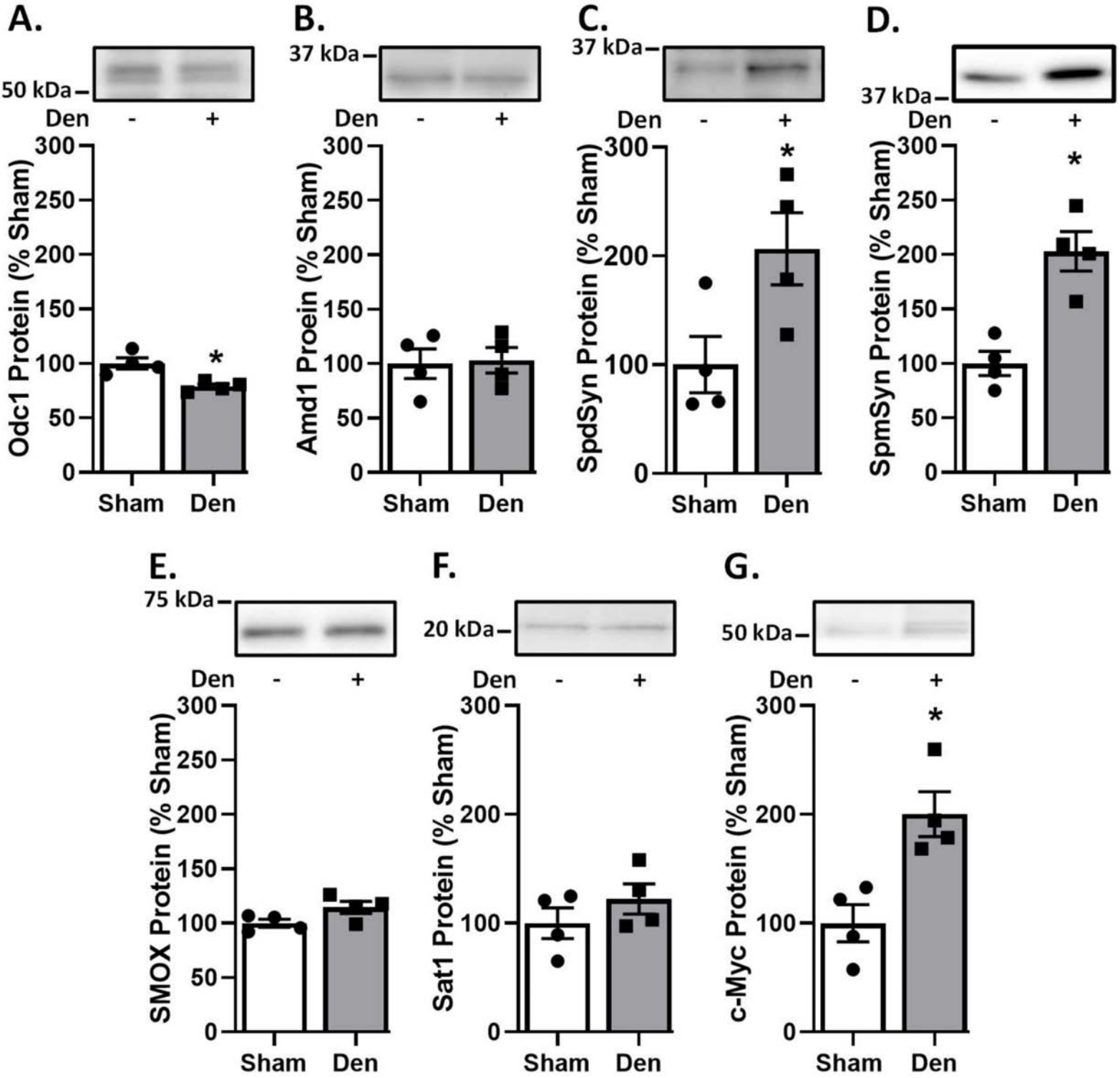
A.
50 kDa
Den - +
Odc1 Protein (% Sham)
300
250
200
150
100
50
0
*
Sham Den
B.
37 kDa
Den - +
Amd1 Proein (% Sham)
300
250
200
150
100
50
0
Sham Den
C.
37 kDa
Den - +
SpdSyn Protein (% Sham)
300
200
100
0
*
Sham Den
D.
37 kDa
Den - +
SpmSyn Protein (% Sham)
300
250
200
150
100
50
0
*
Sham Den
E.
75 kDa
Den - +
SMOX Protein (% Sham)
300
250
200
150
100
50
0
Sham Den
F.
20 kDa
Den - +
Sat1 Protein (% Sham)
300
200
100
0
Sham Den
G.
50 kDa
Den - +
c-Myc Protein (% Sham)
300
200
100
0
*
Sham Den

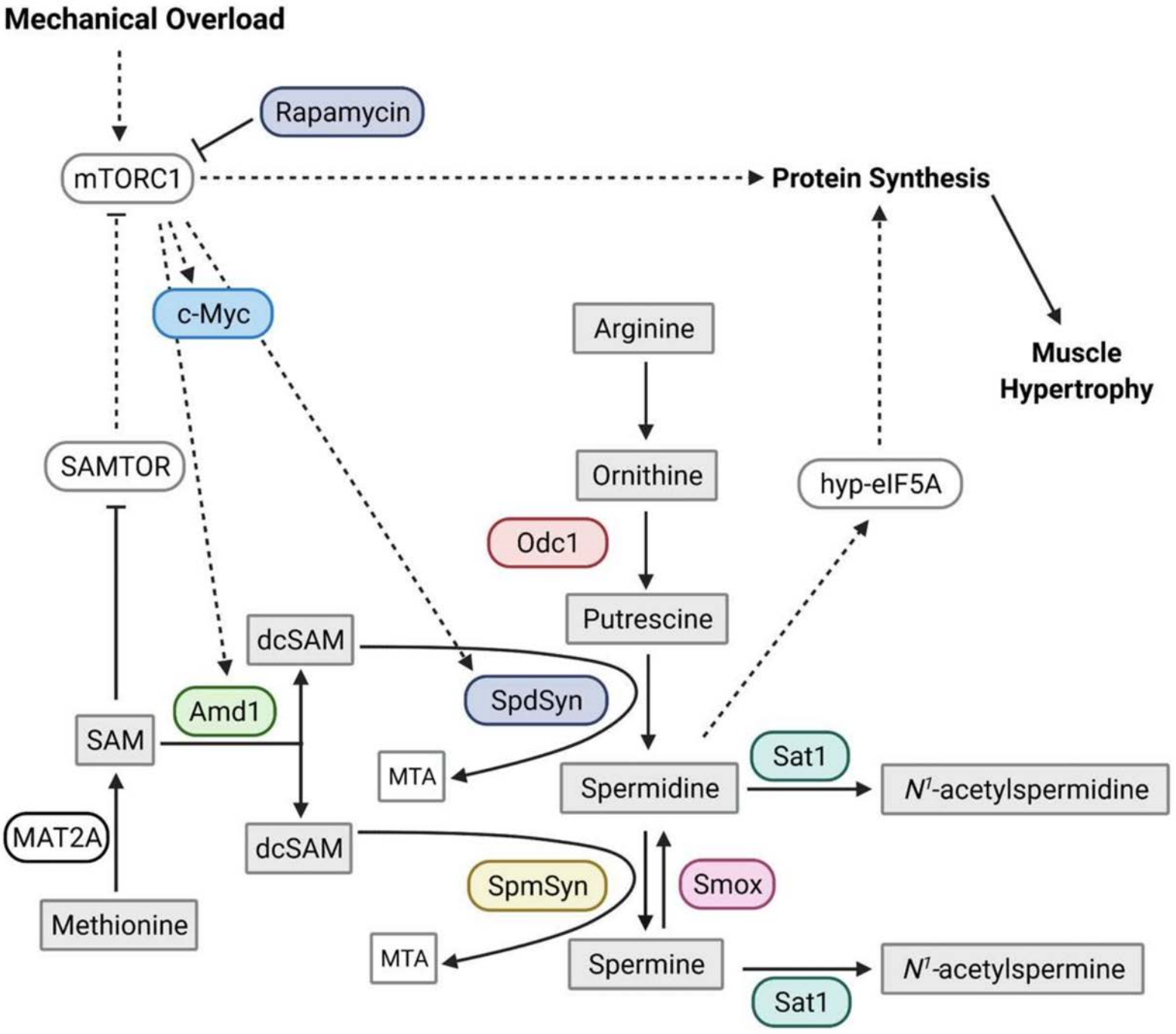
Mechanical Overload
Rapamycin
mTORC1
Protein Synthesis
Muscle Hypertrophy
c-Myc
Arginine
SAMTOR
Ornithine
hyp-eIF5A
Odc1
Putrescine
dcSAM
SpdSyn
Amd1
SAM
MTA
Spermidine
Sat1
N1-acetylspermidine
MAT2A
dcSAM
SpmSyn
Smox
Methionine
MTA
Spermine
N1-acetylspermine
Sat1